Published in final edited form as:
Int J Pharm. 2008 September 1; 361(1-2): 19–25. doi:10.1016/j.ijpharm.2008.05.001.

In Vitro Plasma Stability, Permeability and Solubility of Mercaptoacetamide Histone Deacetylase Inhibitors

Roula Konsoula and **Mira Jung**†
Department of Radiation Medicine, Lombardi Cancer Center, Georgetown University Medical Center, Washington, DC, 20057

Abstract

Histone deacetylase inhibitors (HDACIs) are emerging as a new class of therapeutic agents with potent antitumor activities in a broad spectrum of human cancers. In this study, the *in vitro* plasma stability, permeability, solubility, and lipophilicity (log*D*) of two mercaptoacetamide-based HDACIs (coded as W2 and S2) were evaluated and compared to Vorinostat (SAHA). The results demonstrated that the compounds manifested high solubility in HCl (pH 1.2) but lower in PBS (pH 7.4) than SAHA. Moreover, mercaptoacetamide-based HDACIs exhibited higher lipophilicity values compared to SAHA. The permeability of these compounds was evaluated using the Caco-2 cell monolayer as a model of the intestinal mucosa. The Caco-2 studies revealed that the compounds S2 and W2 are highly permeable with apparent permeability coefficients (P_{app}) in the apical to basolateral direction of 7.33×10^{-6} and 15.0×10^{-6} cm/s, respectively. The *in vitro* stability was determined in human, mouse, porcine and rat plasma. Data showed that the compound W2 is more stable in human and rat plasma and the S2 is more stable in all plasma species than SAHA. Taken together, these results indicate that the mercaptoacetamide-based HDACIs possess favorable solubility, lipophilicity, permeability and plasma stability features.

Keywords

Histone deacetylase inhibitors (HDACIs); Mercaptoacetamides; Solubility; Permeability; Lipophilicity; Plasma Stability

1. Introduction

Epigenetic modifications are increasingly recognized to play significant roles in both normal cellular physiology and disease processes, particularly in cancer where aberrant gene expression has long been associated with the pathogenesis of diseases. The histone acetylation status, one of the major groups mediating epigenetic modifications, is determined by the opposing actions of histone acetyltransferases (HATs) and histone deacetylases (HDACs). HAT inactivation has been linked to oncogenesis and experimental evidence suggests that the aberrant HDAC activity leads to the transcriptional repression of specific tumor suppressor genes, thus contributing to tumor formation (Marks et al., 2001; Karagiannis et al., 2006).

†To whom correspondence and reprints should be addressed: Mira Jung, Division of Radiation Research, Department of Radiation Medicine, The Research Building, Room E-211, Georgetown University School of Medicine, Box 571482, 3970 Reservoir Road, NW, Washington, DC 20057-1482, USA. Tel.: 202-687-8352. FAX: 202-687-7529. E-mail: jungm@georgetown.edu.

Actions of HDAC inhibitors (HDACIs) often result in cell cycle arrest, differentiation and apoptosis in numerous transformed cell lines in culture and *in vivo* (Johnstone, 2002; McLaughlin and La Thangue, 2004; Minucci and Pelicci, 2006). Therefore, the development of HDACIs as therapeutic agents for cancer treatment has recently been intensified.

Nevertheless, Vorinostat known as SAHA (suberoylanilide hydroxamic acid) that recently has been approved by FDA for the treatment of cutaneous T-cell lymphoma (CTCL) is not an ideal drug due to its low solubility and permeability classification (class IV), according to the Biopharmaceutical Classification System (BCS), and short half-life in clinical trials (half-life of 120 minutes for oral administration versus 40 minutes for intravenous) (Kelly et al., 2005). Moreover, HDACIs with substantially longer half-lives, such as MS-275 with a half-life of up to 80 hours, display higher toxicity profiles (Ryan et al., 2005). Additionally, Valproic acid binds to serum proteins (up to 90% of the absorbed drug) and exhibits low potency (Minucci et al., 2006).

Growing evidence has also revealed that the hydroxamate group is associated with low oral bioavailability, poor *in vivo* stability, and undesirable side effects (Mulder et al., 1983; Vassiliou et al., 1999; Suzuki et al., 2005). It has also been shown that the hydroxamate type inhibitor Batimastat promoted liver metastasis in a tumor free mouse model (Kruger et al., 2001). As such, it has become increasingly important to identify replacement groups that exhibit strong inhibitory action against HDACs. Therefore, the design of novel HDACIs with more desirable properties than the existing ones is required.

The identification and optimization of the properties of a compound in the early stage of the drug discovery process are of crucial importance. A successful drug-lead candidate must possess favorable characteristics, including potency and selectivity to the biological target, minimal toxicity, good stability and physicochemical profile, and desirable absorption, distribution, metabolism and excretion properties. The evaluation of the drug-like properties is a useful tool in the selection of a lead compound for further preclinical investigation and the design of more potent and less toxic compounds.

Previously, we have designed a number of mercaptoacetamide-based HDACIs (Chen et al., 2005) and tested for their antitumor activities in a human prostate tumor xenograft model. Two compounds (Figure 1), 6-[(2-mercaptoacetyl)amino-N-8-quinolinyl-hexamide coded as W2, and N-[5-[(4-Dimethylaminobenzoyl)amino]pentyl]-2-mercaptoacetamide as S2, conferred significant tumor regression. Therefore, in the present study, we evaluated the properties of the two mercaptoacetamide-based HDACIs by measuring the level of intestinal absorption, aqueous and lipid solubility, and *in vitro* plasma stability and compared them to the hydroxamate-based HDACI SAHA.

2. Materials and Methods

Materials

Caco-2 cells were obtained from the Tissue Culture Shared Resources of the Lombardi Comprehensive Cancer Center. Dulbecco's Modified Eagle Medium (DMEM) containing D-glucose (4.5 g/l) and L-glutamine, Hanks' balanced salt solution (HBSS), 0.05% trypsin-EDTA, phosphate buffered saline (PBS, pH 7.4), penicillin-streptomycin (10000 U/ml- 10000 μg/ml), non-essential amino acids(NEAA), fetal bovine serum were purchased from Invitrogen (Carlsbad,CA). 1-Octanol (Chromasolv® for HPLC), acetonitrile (LC-MS Chromsolv® for HPLC), lucifer yellow CH dipotassium salt were obtained from Sigma Chemical Company (St. Louis, MO). Spin-X® centrifuge tube filters and transwell® inserts (12-well plates, 12 mm diameter, 1.12 cm^2 surface area) with a permeable polycarbonate

membrane (3.0 μm pore size) were purchased from Costar (Cambridge, MA). Plasma from human, mouse, rat, porcine was supplied by Sigma Chemical Company (St. Louis, MO).

2.2. Cell culture

Caco-2 cells were grown in DMEM supplemented with 10% fetal bovine serum, 1% (NEAA), 1% glutamine, 50 U/ml penicillin and 50 μg/ml streptomycin in an atmosphere of 5% CO_2 and 100% humidity in air. In the present study, Caco-2 cells were used between passages 30–40. For transport experiments, 5×10^5 cells/insert were seeded on polycarbonate filter inserts and cultured as previously described by Konsoula and Barile (2005). Briefly, cells were allowed to grow and differentiate on inserts for 21–28 days. The medium was replenished every second day. The volumes on the apical (insert) and basolateral (well) compartments were maintained at 0.5 and 1.5 ml, respectively. The cell monolayer integrity was monitored by measuring the transepithelial electrical resistance (TEER) with a Millicell-ERS Volt/ohmmeter (Millipore Corp., Bedford, MA). TEER values grater than 400 Ω cm^2 were used for the transport studies.

2.3. Transport studies

The TEER of the Caco-2 monolayer was measured before and after the transport experiments. Lucifer yellow (LY) was used as a negative control compound to assess the integrity of the monolayer. The transport assays were performed in Hanks' balanced salt solution (HBSS) buffer (pH 7.4) at 37°C using a shaking water bath. Prior to conducting all experiments, the monolayer was incubated with HBSS buffer for 15 min. The test compounds were dissolved in HBSS buffer to a final concentration of 150 nmol/ml. Permeability values were determined from both apical to basolateral (AP to BL) and basolateral to apical (BL to AP) sides of the cell monolayer. For absorptive (AP to BL) transport experiments, the test compound (0.5 ml, in HBSS) was placed in the donor (AP) compartment, and the HBBS buffer (1.5 ml) was added to the receiver (BL) chamber. For secretive (BL to AP) transport studies, the test compound (1.5 ml in HBSS buffer) was applied in the donor (BL) chamber, and the HBSS buffer (0.5 ml) was added to the receiver (AP) side. At appropriate time intervals (0, 15, 30, 45, 60, 90, 120, 180 min), aliquots (200 μl) were removed from each receiver compartment, and the amounts withdrawn were replaced with equal volumes of HBSS buffer. The dilution was taken into consideration for the transport calculations. The samples were analyzed by high performance liquid chromatography (HPLC). The data represent the mean of three independent experiments.

2.4. Apparent permeability coefficient (P_{app})

The apparent permeability coefficient values (P_{app}, cm/sec) were calculated from the following equation (Artursson, 1991; Meaney and O'Driscoll, 1999):

$$\text{Papp} = \frac{Vr}{A\,x\,Co}\,x\,\frac{dC}{dt} \quad (1)$$

where dC/dt (nmol/ ml sec) is the rate at which the compound appears in the receiver side-found from the slope of the concentration vs. time graph, V_r is the volume in the receiver chamber (ml), A is the surface area of the filter membrane (cm^2) and C_o is the initial concentration in the donor chamber (nmol/ml).

2.5. Solubility determination

The solubility of the test compounds in phosphate buffered saline (PBS, pH 7.4) and hydrochloric acid (HCl, pH 1.2) was determined by the shake flask method (Löbenberg et al., 2000). Excess amounts of the test compounds were placed in screw-capped vials containing 2 ml of PBS or HCl. The suspensions were vortexed for 2 min and kept in a shaking water bath maintained at 37°C. At appropriate intervals, a portion of the samples (200 μl) was removed and transferred into the filter inserts of the centrifuge tubes. After centrifugation at 14,000 rpm

for 10 min, the filtrates were diluted with acetonitrile (1:1, v/v) and then analyzed by HPLC. The values represent the mean of three independent experiments.

2.6. Octanol-PBS partition coefficient (log*D*)

The partition coefficient (log*D*) of the test compounds between Octanol and phosphate buffered saline (PBS, pH 7.4) was determined at 37°C by the traditional shake flask method (Avdeef et al., 2002; Leo et al., 1971). Weighed amounts (1 mg) of the test compounds in PBS (1 ml) were shaken for 1 h with Octanol (1 ml) to reach equilibrium, and the two phases were separated by centrifugation at 10,000 rpm for 10 min. The concentrations of the test compounds in the Octanol and the PBS layers were determined by HPLC. The log*D* was calculated by employing the following equation:

$$\log D = \log AUC_{oct} / AUC_{buffer} \quad (2)$$

where AUC_{oct} /AUC_{buffer} refers to the areas under the curve for the Octanol and the PBS layers, respectively. Determinations were performed in triplicate for each compound.

2.7. *In* vitro stability in plasma

The *in* vitro stability of the test compounds was studied in human, mouse, porcine and rat plasma. The plasma from the different species was diluted to 80% with 0.05 M PBS (pH 7.4) at 37°C. The reactions were initiated by the addition of the test compounds to 1 ml of preheated plasma solution to yield a final concentration of 200 μM. The assays were performed in a shaking water bath at 37°C and conducted in triplicate. Samples (50 μl) were taken at 0, 15, 30, 45, 60, 90 min and added to 200 μl acetonitrile in order to deproteinize the plasma. The samples were subjected to vortex mixing for 1 min and then centrifugation at 4°C for 15 min at 14,000 rpm. The clear supernatants were analyzed by HPLC. The values represent the mean of three independent experiments.

The *in* vitro plasma half life ($t_{1/2}$) was calculated using the expression $t_{1/2}=0.693/b$, where *b* is the slope found in the linear fit of the natural logarithm of the fraction remaining of the parent compound vs. incubation time.

2.8. HPLC analysis

The samples were analyzed by HPLC. LC was performed using a Shimadzu LC-20AD HPLC system consisting of a UV/VIS detector (SDP-20AV), degasser (DGU-20A), and an autosampler (SIL-HT_A). LC was carried out on an analytical column (Phenomenex Luna C18 (2); 3.0 μm, 100 by 4.6 mm). The mobile phase consisted of acetonitrile-water with 0.1% acetic acid (40:60, v/v) (for the compound S2 and SAHA) or acetonitrile-water with 0.1% acetic acid (50:50, v/v) (for the compound W2). The compound W2 was detected at 330nm while the compound S2 and SAHA were detected at 260nm. The injection volume was 20 μl and the flow rate was 1 ml/min. Standard curves were constructing by plotting the peak areas vs. diluted concentrations (in a range of 0.01–1000 μg/ml) of stock solutions of the compounds.

2.9. Statistical analysis

All experiments were performed at least in triplicate. Results are presented as mean values ± S.E.M. Statistical significance was performed using the Student's two-tailed paired *t*-test and determined at the 95% confidence limit.

3. Results

3.1. Solubility studies at pH 1.2 and 7.4

Drug solubility is one of the core factors, which affect the movement of a drug from the site of administration into the bloodstream. It is widely acknowledged that insufficient drug solubility can lead to poor oral absorption (Zhao et al., 2002). In the present study, the solubility of the mercaptoacetamide-based HDACIs and SAHA was conducted at 37°C in HCl (pH 1.2) and PBS (pH 7.4). Figure 2 illustrates the results from the solubility studies over a period of 24 h. It has been shown that orally administered drugs are well absorbed if they have a minimum solubility of 10 μg/ml and log$P \geq 2$ (Wakita et al., 1986). The experimental data revealed that the tested HDACIs demonstrated good solubility (>10 μg/ml) under conditions simulating the acidic environment of the stomach (pH 1.2) and the neutral environment of the small intestine (pH 7.4). Moreover, the two compounds showed statistically higher solubility profiles in HCl (pH 1.2) and lower solubility in PBS (pH 7.4) compared to SAHA (paired Student's *t*-test, $p<0.05$). This observation was probably related to the fact that the hydroxamic acid of SAHA was unstable under the acidic conditions and overtime underwent acid hydrolysis to form the carboxylic acid.

3.2. Calculation of Octanol-PBS (log*D*) partition coefficient

The Octanol-PBS partition coefficient (log*D*) values are listed in Table 2. The compounds W2 and S2 exhibited higher lipophilicity values than SAHA with log*D* of 2.64, 2.19 and 1.46, respectively. The data suggests that there is a correlation between chemical structure and lipophilicity. Notably, both mercaptoacetamide-based HDACIs predominately distributed into the non-aqueous environment (Octanol phase) and, therefore, they can be expected to penetrate the biological membranes at high potency.

3.3. Transport experiments across Caco-2 monolayer

The human colonic adenocarcinoma Caco-2 cell culture is the most widely employed *in vitro* model that mimics the absorptive properties of the intestinal epithelium (Knipp et al., 1997; Yamashita et al., 2000). The Caco-2 cells spontaneously differentiate in culture into polarized cell monolayers and develop morphological features such as tight junctions, microvilli, and brush border enzymes found in enterocytes (Delie and Rubas, 1997). Therefore, the transport of compounds was measured to evaluate their intestinal permeation. Experiments were conducted at 37°C, and measurements were performed over a 3 h incubation period. Figure 3 summarizes the kinetics of the compound uptakes by Caco-2 cells. The results indicate that the transport of the HDACIs across Caco-2 brush-border membranes took place in both apical to basolateral (AP to BL) and basolateral to apical (BL to AP) directions. In every instance (Figure 3, upper panel), the BL to AP flux was greater than in the other direction (statistically significant, $p<0.05$ based on paired Student's *t*-test), indicating the involvement of an efflux pump which removed the compounds from inside the cell membranes. Moreover, the data demonstrate that the compounds and SAHA showed linear transport across the Caco-2 cell line over a 3 h period. However, as shown in Figure 3 (lower panel), both apical and basolateral transport of the compound W2 was significantly higher than the compound S2 and SAHA ($p<0.05$, paired Student's *t*- test).

Table 2 summarizes the apparent permeability coefficients (P_{app}) values for the permeation of the compounds across Caco-2 cell monolayers in the AP to BL and BL to AP directions. The AP to BL P_{app} has been widely used as a potential predictor of oral absorption. As can be seen, the descending order of the absorption was W2>S2>SAHA within 3 h incubation period. Significant differences in P_{app} values for basal to apical and apical to basal were detectable for compounds W2 (BL to AP, 24.7±0.12; AP to BL 15.0±0.2; $p<0.05$), S2 (BL to AP, 10.0±0.4; AP to BL 7.33±0.3; $p<0.05$), and SAHA (BL to AP, 6.33±0.3; AP to BL 3.00±0.2; $p<0.05$).

The P_{app} ratio values (P_{app} BL to AP/ P_{app} AP to BL) of the compounds W2, S2 and SAHA were 1.64, 1.36 and 2.11, respectively. Thus, the efflux ratios correlate well with the known expression of P-glycoprotein on the apical side of the Caco-2 cell line (Hunter et al., 1993).

3.4. *In vitro* plasma stability studies

The stability profiles of the compounds and SAHA in human, mouse, porcine and rat plasma are presented in Figure 4. Statistical analysis revealed that there is a significant difference in the concentration of the compound S2 in the plasma of mouse vs. porcine and mouse vs. human (paired Student's *t*-test, $p<0.05$). The plasma concentration-time data of the compound W2 in human vs. mouse, human vs. rat and porcine vs. rat was significant different from each other (paired Student's *t*-test, $p<0.05$). As comparison, the corresponding plasma concentration-time profile of SAHA was investigated. Significant differences in SAHA concentrations were revealed in mouse vs. rat plasma and mouse vs. porcine plasma (paired Student's *t*-test, $p<0.05$).

Comparison between the *in vitro* half-lives ($t_{1/2}$) of the compounds and SAHA in different plasma species is presented in Table 3. The compound S2 displayed far longer stability in all plasma species as compared to SAHA. For the compound W2, the *in vitro* half-lives in human and rat plasma were found to be 79 and 92 min which were longer than SAHA (75 and 86 min, respectively).

4. Discussion

Characterization of the chemical and biochemical properties of a compound in the early stage of the drug discovery process is important. The determination of the physicochemical properties as well as estimation of absorption, distribution, metabolism are important in the lead compound nomination. Such information can help to design more active compounds and thereby cut down substantially on time and costs between discovery and clinical trials.

In this study, we elucidated the physicochemical attributes of novel mercaptoacetamide-based HDACIs. Since aqueous and lipid solubility demonstrate a reverse relationship, a balance between these aspects is required for optimal absorption. Camenisch et al., (1998) were able to demonstrate that the permeability of a molecule increases directly with its lipophilicity until it reaches a plateau at log$P\geq 2$. Hydrophobic compounds (log$P>4$) tend to have low aqueous solubility and distribute at a slower rate from the lipid membranes to the extracellular fluid (Artursson et al., 2001). The experimental data demonstrated that these mercaptoacetamide-based HDACIs have higher solubility in acidic (HCl, pH 1.2) but lower solubility in neutral environment (PBS, pH 7.4) as compared to SAHA. This observation can be explained by the fact that the hydroxamic acid of SAHA was unstable under the acidic conditions and overtime hydrolyzed to form the carboxylic acid. Furthermore, the data revealed that the mercaptoacetamide-based HDACIs display higher lipophilicity values as compared to SAHA. Therefore, these findings indicate that there is a relationship between chemical structure and lipophilicity. Indeed, both mercaptoacetamides showed a tendency of being predominately distributed into the Octanol layer, behaving as essentially non-polar compounds.

The biopharmaceutics classification system (BCS) outlines the parameters for predicting bioavailability of drugs based on their aqueous solubility and intestinal permeability (Amidon et al., 1995; Kasim et al., 2004). The BCS Guidance has classified drugs into the following four groups: Class 1: high solubility-high pemeability; Class 2: low solubiity-high permeability; Class 3: high solubility-low permeability; Class 4: low solubility-low permeability. Using the human intestinal Caco-2 cell line, the three model compounds and SAHA were classified for their permeability. According to the experimental data described in this study, the compounds S2 and W2 cross the transepithelial layer very quickly at 37°C with permeability coefficients P_{app} (AP to BL) of 7.33 to 15.0×10^{-6} cm/s, respectively. Artursson

et al. (1991, 2001), has established the correlation between the transport by Caco-2 cells and the fraction absorbed *in vivo.* Compounds completely absorbed in humans were found to have permeability coefficients (P_{app} AP to BL > 1×10^{-6} cm/s), whereas incompletely absorbed drugs had low permeability coefficients (P_{app} AP to BL < 1×10^{-7} cm/s) in Caco-2 cells. Based upon comparison to SAHA (P_{app} AP to BL = 3×10^{-6} cm/s), the compounds W2 and S2 bearing the mercaptoacetamide end moiety are expected to be readily absorbed *in vivo*.

The screening of compounds stability in plasma provides useful information about possible liabilities of drug candidates. Unstable compounds tend to exhibit rapid clearance, short half-lives and consequently poor *in vivo* activity (Di et al., 2005). Compounds with certain functional groups including amides, esters, lactams, sulfonamides, have a tendency to undergo hydrolysis by plasma enzymes. It has been shown that there are significant species variations regarding the elimination kinetics of several drugs (Shukla et al., 2007). Szotakova et al., (2004) have demonstrated marked differences in the *in vitro* activities of biotransformation enzymes among animal species. Plasma from human, mouse, porcine and rat was used in these studies in order to evaluate the *in vitro* stability of the HDACIs. Our findings reveal that compound S2 exhibited longer half-lives in all plasma species as compared to SAHA (Table 3). The compound W2 was more stable in human and rat plasma (79 and 92 min, respectively) than SAHA (75 and 86 min, respectively).

Several reports have correlated the hydroxamate group with poor solubility, unfavorable pharmacokinetics including glucuronidation, sulfation, enzymatic hydrolysis and therefore short *in vivo* half life (Mulder et al., 1983; Vassiliou et al., 1999; Pikul et al., 2001; Suzuki et al., 2005). The results of our study suggest that the hydroxamic acid end moiety of SAHA might be associated with moderate physicochemical properties and overall pharmacokinetic behavior compared to mercaptoacetamides. The thiol functionality has been shown to be a good replacement for hydroxamic acid, since zinc ion is highly thiophilic and thiol derivatives have been documented to inhibit zinc dependent enzymes including matrix metalloproteinases and angiotensin converting enzyme (Jung et al., 1999; Michaelides et al., 2001; Pikul et al., 2001; Remiszewski et al., 2002 Suzuki et al., 2004). Also it has been demonstrated that the disulfide bond in the depsipeptide, FK228, was reduced within the cells, releasing the zinc binding thiol moiety and resulting in HDAC inhibition (Furumai et al., 2002). Anandan et al., (2005) have shown that substituting the hydroxamate moiety with the mercaptoamide functionality inhibited HDAC activity at low micromolar concentration levels. Therefore, it may be possible that thiols inhibit HDAC activity by forming a covalent disulfide bond with the cysteine residues on these enzymes is a mechanism of action of these compounds associated with their physicochemical properties and pharmacokinetic behavior.

In summary, we have demonstrated that the mercaptoacetamide-based HDACIs possess favorable solubility, lipophilicity, permeability and plasma stability features as compared to recently FDA approved drug Vorinostat (SAHA). Based on these findings, we assume that these compounds could sufficiently be absorbed by the intestinal tract. However, further studies are needed in order to determine the pharmacokinetic disposition of these compounds.

Acknowledgements

We thank Gene therapy pharmaceuticals for providing the compounds and Dr. Milton Brown for sharing the equipment and chemical reagents. This work was supported by the grant, P02 CA74175 (to A.D. and M.J.) from the National Cancer Institute.

References

Amidon GL, Lennermas H, Shah VP, Crison JR. A theoretical basis for a biopharmaceutical drug classification: the correlation of in vitro drug product dissolution and in vivo bioavailability. Pharm. Res 1995;12:413–420. [PubMed: 7617530]

Anandan SK, Ward JS, Brokx RD, Bray MR, Patel DV, Xiao XX. Mercaptoamide-based non-hydroxamic acid type histone deacetylase inhibitors. Bioorg. Med. Chem. Lett 2005;15:1969–1972. [PubMed: 15808449]

Artursson P, Karlson J. Correlation between oral drug absorption in humans and apparent drug permeability coefficients in human intestinal epithelial (Caco-2) cells. Biochem. Biophys. Res. Commun 1991;175:880–885. [PubMed: 1673839]

Artursson P, Palm K, Luthman K. Caco-2 monolayers in experimental and theoretical predictions of drug transport. Ad. Drug Delivery Rev 2001;46:27–43.

Avdeef A, Twsta B. Physicochemical profiling in drug research: a brief survey of the state of the art of experimental techniques. Cell Mol. Life Sci 2002;59(10):1681–1689. [PubMed: 12475179]

Camenisch G, Alsenz J, Van De Waterbeemd H, Folkers G. Estimation of permeability by passive diffusion through Caco-2 cell monolayers using the drugs' lipophilicity and molecular weight. Eur. J. Pharm. Sci 1998;6:321–329.

Chen B, Petukhov PA, Jung M, Velena A, Eliseeva E, Dritschilo A, Kozikowski AP. Chemistry and biology of mercaptoacetamides as novel histone deacetylase inhibitors. Bioorg. Med. Chem. Lett 2005;15:1389–1392. [PubMed: 15713393]

Delie F, Rubas W. A human colonic cell line sharing similarities with enterocytes as a model to examine oral absorption: advantages and disadvantages of the Caco-2 model. Crit. Rev. Ther. Drug Carrier Syst 1997;14:221–286. [PubMed: 9282267]

Di L, Kerns EH, Hong Y, Chen H. Development and application of high throughput plasma stability assay for drug discovery. Int. J. Pharm 2005;297(1–2):110–119. [PubMed: 15876500]

Furumai R, Matsuyama A, Kobashi N, Lee KH, Nishiyama M, Nakajima H, Tanaka A, Komatsu Y, Nishino N, Yoshida M, Horinouchi S. FK228 (Depsipeptide) as a neutral prodrug that inhibits class I histone deacetylases. Cancer Res 2002;62:4916–4921. [PubMed: 12208741]

Hunter J, Jepson MA, Tsuruo T, Simmons NL, Hirst BH. Functional expression of P-glycoprotein in apical membranes of human intestinal Caco-2 cells. Kinetics of vinblastine secretion and interaction with modulators. J. Biol. Chem 1993;268:14991–14997. [PubMed: 8100817]

Johnstone RW. Histone-deacetylase inhibitors: novel drugs for the treatment of cancer. Nat. Rev. Drug Discov 2002;1:287–299. [PubMed: 12120280]

Jung M, Brosch G, Kölle D, Scherf H, Gerhäuser C, Loidl P. Amide analogues of Trichostatin A as inhibitors of histone deacetylase and inducers of terminal cell differentiation. J. Med. Chem 1999;42:4669–4679. [PubMed: 10579829]

Karagiannis TC, El-Osta A. The paradox of histone deacetylase inhibitor-mediated modulation of cellular responses to radiation. Cell Cycle 2006;5(3):288–295. [PubMed: 16418577]

Kasim NA, Whitehouse M, Ramachandran C, Bermejo M. Molecular properties of WHO and provisional biopharmaceutical classification. Mol. Pharm 2004;1:85–96. [PubMed: 15832504]

Kelly WK, O'Connor OA, Krug ML, Chiao JH, Heaney M, Curley T, MacGregore-Corteli B, Tong W, Secrist JP, Schwartz L, Richardson S, Chu E, Olgac S, Marks PA, Scher H, Richon VM. Phase I study of an oral histone deacetylase inhibitor, suberoylanilide hydroxamic acid, in patients with advanced cancer. J.Clin. Oncol 2005;23(17):3923–3931. [PubMed: 15897550]

Knipp GT, Ho NF, Barsuhn CL, Borchardt RT. Paracellular diffusion in Caco-2 cell monolayers: effect of perturbation on the transport of hydrophilic compounds that vary in charge and size. J. Pharm. Sci 1997;86:1105–1110. [PubMed: 9344165]

Konsoula R, Barile F. Correlation of in vitro cytotoxicity with paracellular permeability in Caco-2 cells. Toxicology in Vitro 2005;19(5):675–684. [PubMed: 15896555]

Kruger A, Soeltl R, Sopov I, Kopitz C, Arlt M, Magdolen V, Harbeck N, Gansbacher B, Schmitt M. Hydroxamate-type matrix metalloproteinase inhibitor batimastat promotes liver metastasis. Cancer Res 2001;15:1389–1392.

Leo A, Hansch C, Elkins D. Partition coefficients and their uses. Chem. Rev 1971;21:525–616.

Löbenberg, R.; Amidon, GL. Solubility as a limited factor to drug absorption. In: Dressman, JB., editor. Oral Drug Absorption, Prediction and Assessment. New York: Marcel Dekker; 2000.

Marks PA, Rifkind RA, Richon VM, Breslow R, Miller T, Kelly WK. Histone deacetylases and cancer: causes and therapy. Nat. Rev. Cancer 2001;1(3):194–202. [PubMed: 11902574]

McLaughlin F, La Thangue NB. Histone deacetylase inhibitors open new doors in cancer therapy. Biochem. Pharmacol 2004;68:1139–1144. [PubMed: 15313411]

Meaney C, O'Driscoll C. Mucus as a barrier to the permeability of hydrophilic and lipophilic compounds in the absence and presence of sodium taurocholate micellar systems using cell culture models. Eur. J. Pharm. Sci 1999;8:167–175. [PubMed: 10379039]

Michaelides MR, Dellaria JF, Gong J, Holms JH, Bouska JJ, Stacey J, Wada CK, Heyman HR, Curtin ML, Guo Y, Goodfellow CL, Elmore IB, Albert DH, Magoc TJ, Marcotte PA, Morgan DW, Davidsen SK. Biaryl ether retrohydroxamates as potent, long- lived, orally bioavailable MMP inhibitors. Bioorg. Med. Chem. Lett 2001;11:1553–1556. [PubMed: 11412979]

Minucci S, Pelicci PG. Histone deacetylase inhibitors and the promise of epigenetic (and more) treatments for cancer. Nat. Rev. Cancer 2006;6:38–51. [PubMed: 16397526]

Mulder GJ, Meerman JH. Sulfation and glucuronidation as competing pathways in the metabolism of hydroxamic acids: the role of N,O- sulfonation in chemical carcinogenesis of aromatic amines. Environ. Health Perspect 1983;49:27–32. [PubMed: 6339226]

Pikul S, Ohler NE, Ciszewski G, Laufersweiler MC, Almstead NG, De B, Natchus MG, Hsieh LC, Janusz MJ, Peng SX, Branch TM, King SL, Taiwo YO, Mieling GE. Potent and selective carboxylic acid-based inhibitors of matrix metalloproteinases. J.Med. Chem 2001;44(16):2499–2502. [PubMed: 11472202]

Remiszewski SW, Sambucetti LC, Atadja P, Bair KW, Cornell WD, Green MA, Howell KL, Jung M, Kwon P, Trogani N, Walker H. Inhibitors of human histone deacetylase: synthesis and enzyme and cellular activity of straight chain hydroxamates. J.Med. Chem 2002;45(4):753–757. [PubMed: 11831887]

Ryan QC, Headlee D, Acharya M, Sparreboom A, Trepel JB, Ye J, Figg WD, Hwang K, Chung EJ, Murgo A, Melillo G, Elsayed Y, Monga M, Kalnitskiy M, Zwiebel J, Sausville EA. Phase I and Pharmacokinetic study of MS-275, a histone deacetylase inhibitor, in patients with advanced and refractory solid tumors or lymphoma. J. Clin. Oncol 2005;23(17):3912–3922. [PubMed: 15851766]

Shukla M, Singh G, Sindhura BG, Telang AG, Rao GS, Malik JK. Comp. Biochem. Physiol 2007;C145:528–532.

Szotakova B, Baliharova V, Lamka J, Nozinova E, Wsol V, Velik J, Machala M, Neca J, Soucek P, Susova S, Skalova L. Comparison of *in vitro* activities of biotransformation enzymes in pig, cattle, goat and sheep. Res. Vet. Sci 2004;76:43–51. [PubMed: 14659728]

Suzuki T, Kouketsu A, Matsuura A, Kohara A, Ninomiya S, Kohda K, Miyata N. Thiol-based SAHA analogues as potent histone deacetylase inhibitors. Bioorg. Med. Chem. Lett 2004;14:3313–3317. [PubMed: 15149697]

Suzuki T, Matsura A, Kouketsu A, Nakagawa H, Miyata N. Identification of a potent non-hydroxamate histone deacetylase inhibitor by mechanism-based drug design. Bioorg. Med. Chem. Lett 2005;15:331–335. [PubMed: 15603949]

Vassiliou S, Mucha A, Cuniasse P, Georgiadis D, Lucet-Levannier K, Beau F, Kannan R, Murphy G, Knaeuper V, Rio MC, Basset P, Yiotakis A, Dive VJ. Phosphinic pseudo-tripeptides as potent inhibitors of matrix metalloproteinases: a structure –activity study. J. Med. Chem 1999;42:2610–2620. [PubMed: 10411481]

Wakita K, Yoshimoto M, Miyamoto S, Watanabe H. A method for calculation of the aqueous solubility of organic compounds by using new fragment solubility constants. Chem. Pharm. Bull 1986;34:4663–4681.

Yamashita S, Furubayashi T, Kataoka M, Sakane T, Sezaki H, Tokuda H. Optimized conditions for prediction of intestinal drug permeability using Caco-2. Eur. J. Pharm. Sci 2000;10(3):195–204. [PubMed: 10767597]

Zhao YH, Abraham MH, Lee J, Hersey A, Luscombe CN, Beck G, Sherborne B, Cooper I. Rate-limited steps of human oral absorption and QSAR studies. Pharm. Res 2002;19:1446–1457. [PubMed: 12425461]

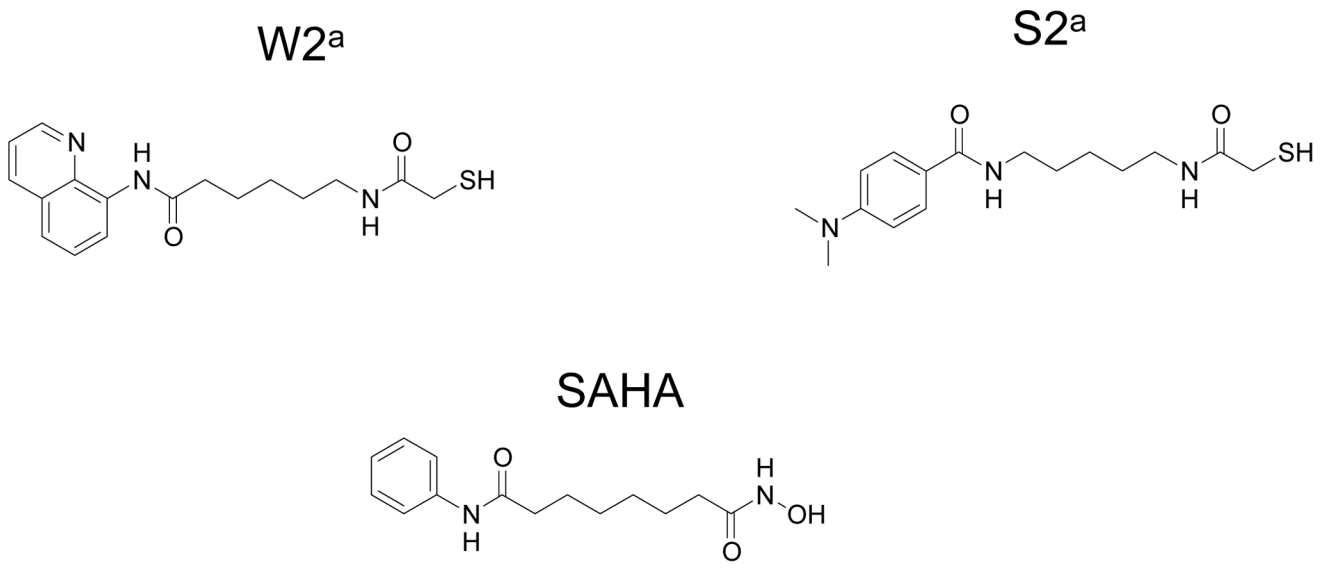

Figure 1.
Chemical Structures of Compounds. [a] taken from Chen et al., 2005.

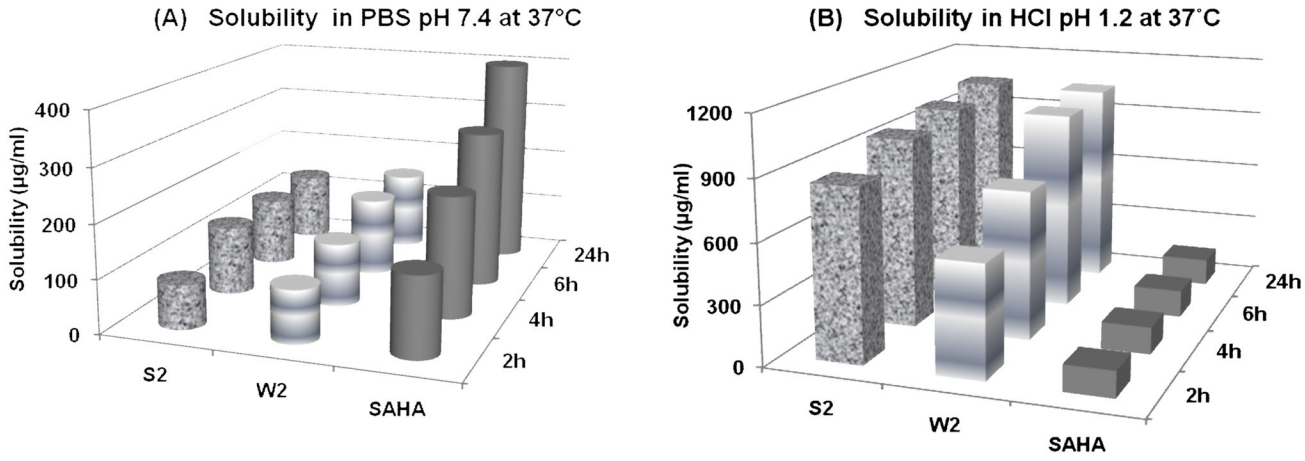

Figure 2.

Solubility profiles of the mercaptoacetamide-based HDACIs and SAHA over a period of 24 h in (A) PBS pH 7.4 at 37°C and (B) HCl pH 1.2 at 37°C. Both compounds demonstrated higher solubility in HCl (pH 1.2) and lower in PBS (pH 7.4) compared to SAHA (paired Student's *t* -test, <0.05).

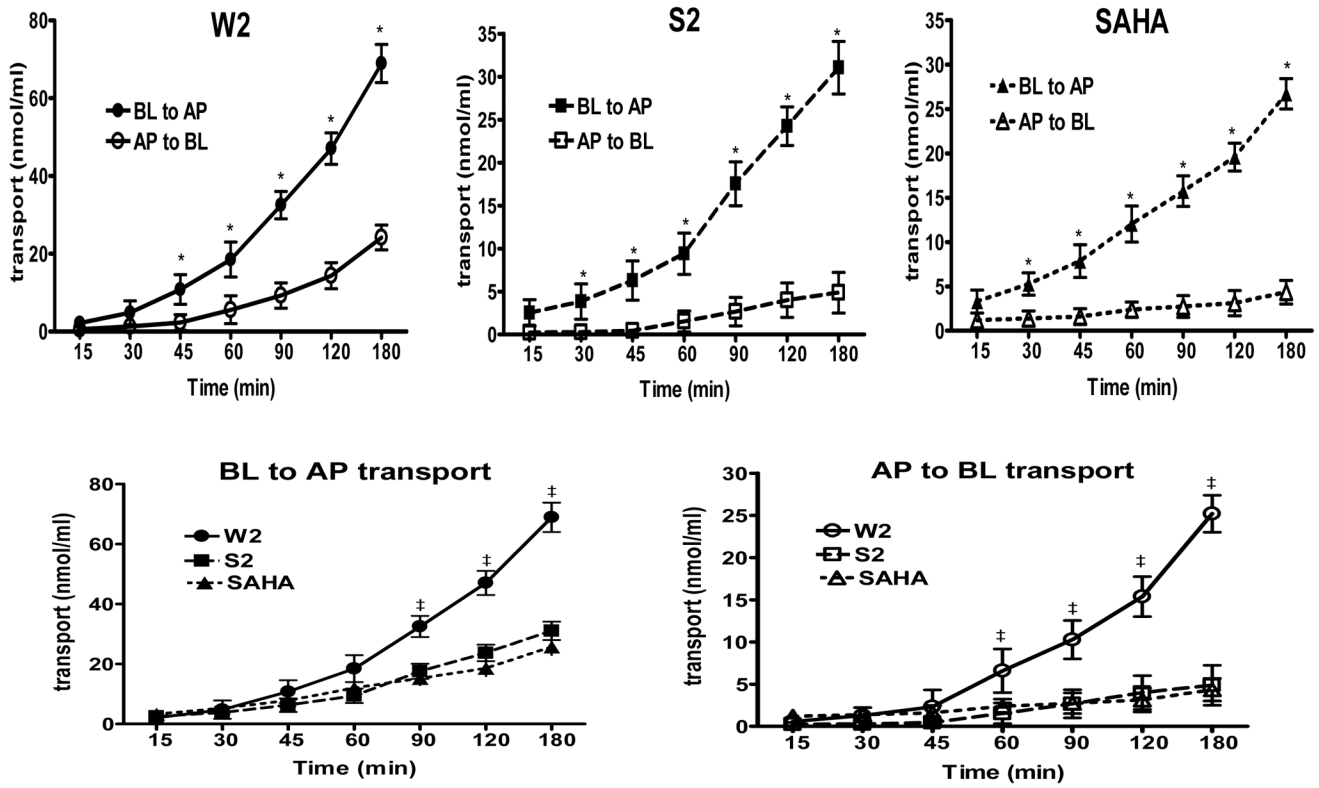

Figure 3.

Time dependent transport of the compounds and SAHA across Caco-2 cells grown on inserts. Transport is expressed as nmol/ml. Data points represent both basolateral to apical (BL to AP) and apical to basolateral (AP to BL) transport. BL to AP transport of W2 (closed circles), S2 (closed squares) and SAHA (closed triangles) is illustrated. AP to BL transport of W2 (open circles), S2 (open squares) and SAHA (open triangles) is displayed. The data points represent the mean values ± S.E.M. of three independent experiments. Statistical analysis was carried out by the paired Student's *t*-test ($p<0.05$). Upper panel, *, BL to AP transport of the compounds and SAHA is significantly higher than AP to BL; $p<0.05$. Lower panel, ‡, the transport of W2 is significant different from SAHA at a level of $p<0.05$.

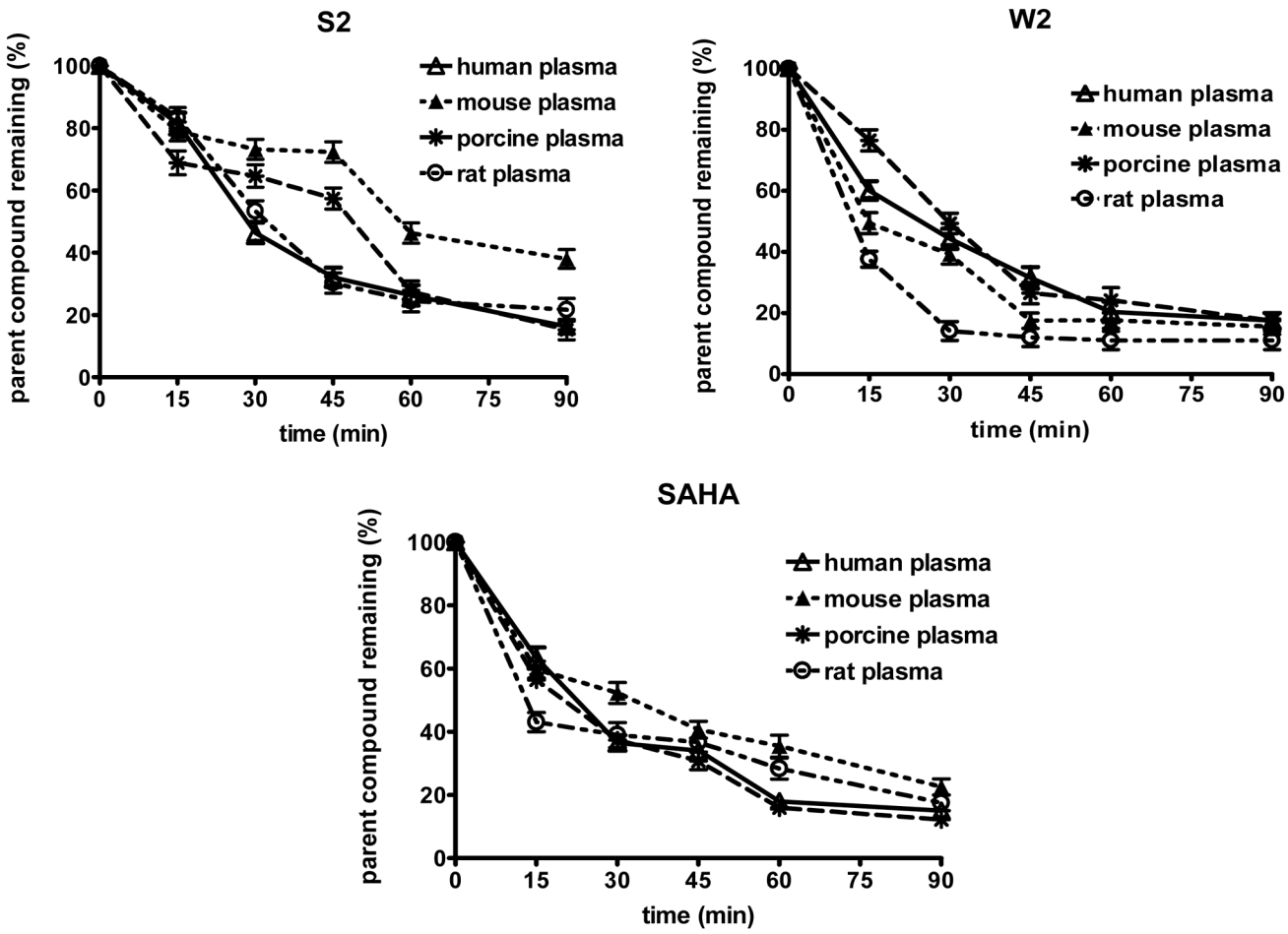

Figure 4.

Stability profiles of the compounds and SAHA obtained in human, mouse, porcine and rat plasma. The values represent the mean ± S.E.M. of three independent experiments. Statistical analysis was performed by using the paired Student's *t*-test at $p<0.05$ level of significance.

Table 1

The Octanol-PBS partition coefficient (log*D*) alues of the compounds and SAHA (± S.E.M.) at 37°C.

Compounds	MW	Log*D*
W2	323.45	2.64±0.1
S2	331.43	2.19±0.1
SAHA	264.15	1.46±0.2

MW: molecular weight in Dalton. log*D* calculated Octanol/PBS partition coefficient.

Table 2

The apparent permeability coefficient (P_{app}, cm/sec) values of the compounds and SAHA across Caco-2 cell monolayers in both apical to basolateral and basolateral to apical directions.

Compounds	P_{app} (cm/sec) × (10^{-6})[a]		P_{app}(BL to Ap) /P_{app}(AP to BL)
	AP to BL	BL to AP	
W2	15.0±0.4[c]	24.7±0.12[b,c]	1.64
S2	7.33±0.3	10.0±0.4[b]	1.36
SAHA	3.00±0.2	6.33±0.3[b]	2.11

[a] Each value represents the mean ± S.E.M. of triplicate independent determinations. AP:apical; BL: basolateral.

[b] Significant difference between BL to AP and AP to BL transport of the compounds and SAHA ($p<0.05$).

[c] Significant difference between transport of compound W2 and SAHA in a particular direction ($p<0.05$).

Table 3

The *in vitro* half-lives ($t_{1/2}$)[a] of the compounds and SAHA in human, mouse, porcine and rat plasma.

Compounds	*In vitro* half-lives (min)			
	Human	Mouse	Porcine	Rat
S2	77	173	89	99
W2	79	58	69	92
SAHA	75	115	87	86

[a] Each value represents the mean ± S.E.M. of triplicate independent determinations.